

# Contents

<b>1</b>	<b>Introduction</b>	<b>2</b>
<b>2</b>	<b>Basic Concept</b>	<b>2</b>
2.1	Pleural Line and Rib . . . . .	2
2.2	B-line . . . . .	2
2.3	A-line . . . . .	3
2.4	B-line Detection Guideline . . . . .	4
<b>3</b>	<b>Image Pre-processing</b>	<b>4</b>
3.1	Fan Area Locating . . . . .	4
3.2	Image Rectification . . . . .	5
3.3	Denoising . . . . .	5
3.4	Normalizing . . . . .	6
<b>4</b>	<b>Image Segmentation</b>	<b>6</b>
4.1	Pleural Line Segmentation . . . . .	6
4.1.1	Region Growing . . . . .	7
4.1.2	Intensity-based Local Peak Searching . . . . .	7
4.2	B-line Detection . . . . .	8
4.3	A-line Detection . . . . .	9
4.4	ABP-line Map Generation . . . . .	10
4.5	B-line Occupancy . . . . .	11
<b>5</b>	<b>Numerical Results</b>	<b>11</b>
5.1	B-line Detection Results . . . . .	11
5.2	Dice Index . . . . .	11
<b>6</b>	<b>Future Perspectives and Summary</b>	<b>12</b>
<b>7</b>	<b>References</b>	<b>12</b>

# B-lines Detection and Evaluation in Thorax Ultrasound Video

Ziyu Shu, Yao Wang, Gabriel Rose

December 16, 2019

**Abstract** Due to its convenient real time, non-invasive detection, lung ultrasound is an excellent diagnostic tool in researches related to pulmonary congestion. However, its objective assessment remains elusive. Currently, the detection and evaluation of pulmonary congestion largely rely on manual detection of B-lines by ultrasound specialists. In this paper, I propose an automatic method to detect B-lines.

**Index terms:** Pulmonary congestion; Oedema; Lung water; Ultrasound; B-lines; Medical image and video processing.

## 1 Introduction

Patients with acute heart failure are usually diagnosed to have pulmonary congestion, which happens at the early stage of the syndrome. The syndrome often has a relative long incubation period, during which there is a gradual accumulation of extravascular lung water (EVLW), a key to detect heart failure. According to [1], lung ultrasound can be used to exam EVLW. In [1], the authors manually evaluate lung ultrasound by counting the number of “B-line”. However, this method may not be accurate and time consuming. Two or more thin B-lines can be falsely combined into one wide B-line as B-lines move with the exhaling and inhaling of our lung. Furthermore, the gains of different lung ultra sound videos may be different, one can easily regard noise pattern as a B-line. The aim of this work is to design a new automatic method to detect and evaluate the lung ultrasound.

## 2 Basic Concept

### 2.1 Pleural Line and Rib

The pleural surface acts as an acoustic reflector that generates the pleural line in ultrasound image. Theoretically pleural line is a thin arch which is the brightest line in the ultrasound image. There are always two ribs adjoining the pleural surface. Rib will absolutely absorb ultrasound, so ribs and the area under the ribs are totally black. When we evaluate the occupancy of B-line, rib spaces should not be considered, as shown in Figure1.

### 2.2 B-line

B-line, which is caused by the ultrasound reflection from tissue with a lot of water, is a vertical, comet-tail artefact arising from the pleural line and spreading up to the edge of screen, as shown in Figure2.

### 2.3 A-line

A-line is just a mirror image of a pleural line, so it always looks like a pleuralline with dark brightness which lies horizontally beneath pleural line. B-line is always brighter than A-line. In that case, once there is an A-line lying on the image, there is no B-line but noise on that column. Sometimes A-line can be very thick, as shown in Figure3 and Figure4.

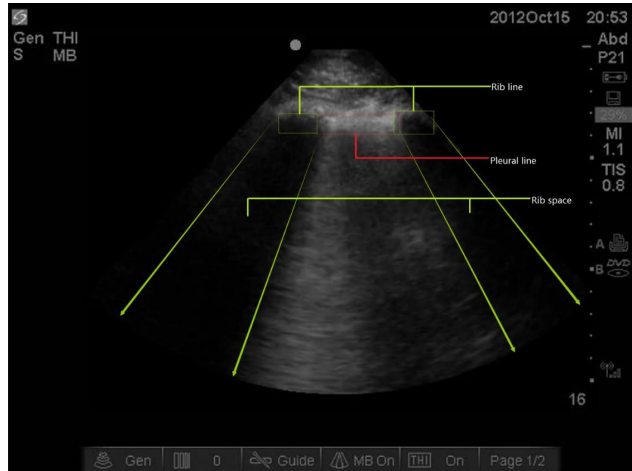


Figure 1: A bright pleural line and two black rib lines with their black rib spaces



Figure 3: A-line

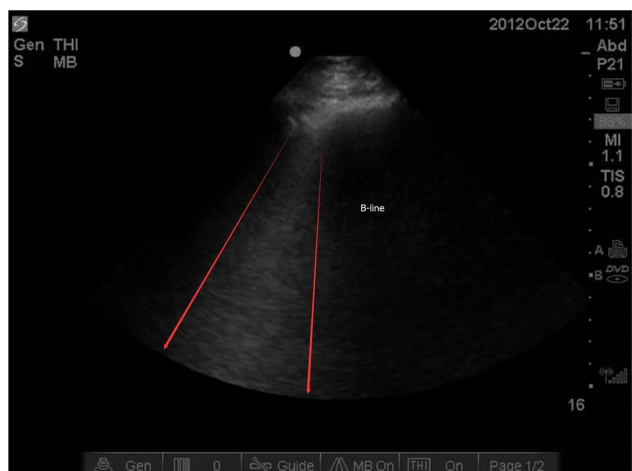


Figure 2: B-line



Figure 4: A-line

## 2.4 B-line Detection Guideline

Based on Kenton et al. [2] and Doctor Gabriel Rose's description, B-lines have the following characteristics:

1. They are fine reverberation artifacts
2. They originate at the pleural line and extend to the lower edge of the screen having no or very little fading
3. They can't coexist with A-lines (A-lines are just the repetitions of pleural lines due to the ultrasound, so their brightness is very low. B-lines' brightness is much higher than A-lines. So, B-lines will absolutely obliterate A-lines)
4. They move synchronously with pleural sliding

To detect and evaluate B-lines, we need both spatial and temporal information. The basic idea is to find pleural line firstly; then search the potential B-lines in pleural space (the area under the pleural line); next check the existence of A-lines; use image processing method to eliminate sparse point; finally compute the occupancy of B-lines from the total video.



Figure 5: Guideline

## 3 Image Pre-processing

In the actual operation, doctors can adjust the gain of probes when generating ultrasound images. The powers of the white noise in different samples are different due to the gain difference, so we need to normalize the samples and eliminate noise before implementing the segmentation methods. In the first section of this chapter, we introduce the fan area locating processing to remove the redundant information out of the ultrasound fan area. The second section focuses on image rectification that transfers the fan-shaped ultrasound image to a standard rectangular image. The last two sections show how to remove

white noise, and normalize the ultrasound image to improve the accuracy of my algorithm.

### 3.1 Fan Area Locating

All the data from Dr.Rose is pre-set to guarantee that the fan areas of ultrasound images are all in the same location. The area out of the fan is totally black. So, it is easy to select the corner points of the fan A, B, C, and D (we can use several frames to make sure they are right). The original frame is shown in Figure6.

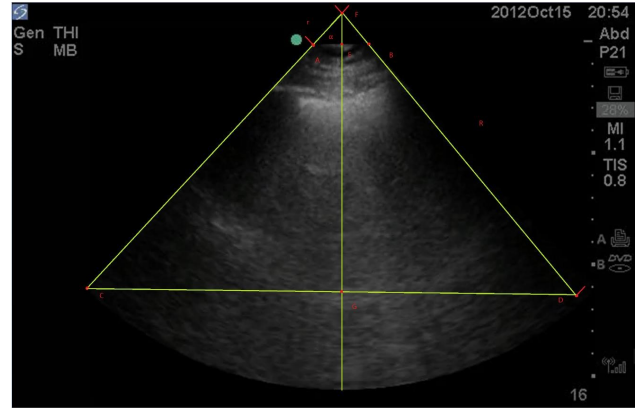


Figure 6: Original Frame

In the figure, FCD is an isosceles triangle, so we can figure out the following solutions:

$$Y_A = Y_E = Y_B \quad (1)$$

$$Y_C = Y_G = Y_D \quad (2)$$

$$Y_F = Y_E = Y_G \quad (3)$$

$$\frac{Y_F - Y_E}{Y_E - Y_G} = \frac{X_E - X_A}{X_G - X_C} \quad (4)$$

$$R = d_{DF} \quad (5)$$

$$r = d_{BF} \quad (6)$$

$$\alpha = 2\tan^{-1}\left(\frac{d_{AE}}{d_{EF}}\right) \quad (7)$$

All the parameters are listed in Table 1.

Table 1: Performance parameters of different innovations

Parameters	Value
Center F	(425,20)
R	481
r	51
$\alpha$	86

### 3.2 Image Rectification

To do the projection along the radial line in the fan-shaped image, we need to transform the fan area to a rectangular area. The outline is shown in Figure7

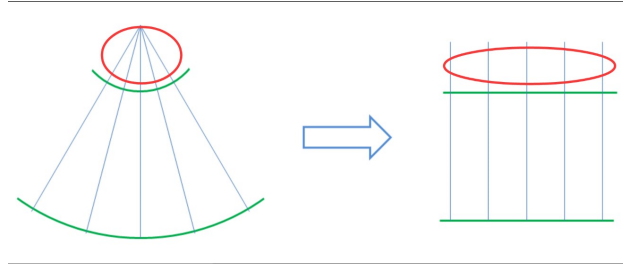


Figure 7: Rectification

In Figure7, we sample the fan area by the radial lines and then transform them into a rectangular form. We can adjust the sample rate to approach higher accuracy. In my algorithm, I sample the fan area by every 1 degree and 481 points for every radial line. In that case, I will get an 87X481 (from  $-43^\circ$  to  $43^\circ$ ) matrix. Using this rectification method will lose the red area of the fan, but it doesn't matter, because there won't be anything valuable in this area. Figure8 is an example.

### 3.3 Denoising

Although ultrasound images can be captured in real-time, low image quality makes it difficult to perform



Figure 8: An example of rectification

segmentation and identification. Among all the noise, speckle noise and white noise are major causes of image quality degradation. For white noise, it makes the total screen brighter and hard to identify. Fortunately, rib space (the area under ribs) is totally black, so we can measure the mean intensity of white noise by averaging the brightness of the rib space. After that, we can get rid of white noise by subtracting the mean white noise intensity from the original frame. This is shown in Figure9.

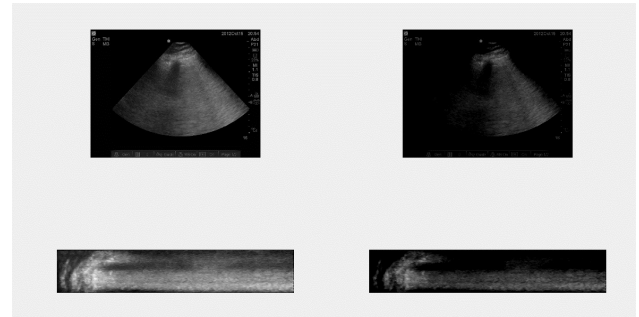


Figure 9: The original noisy frame (left) and the denoised frame (right)

For speckle noise, it is inherently generated from mechanism of ultrasound image system and the motion of our body tissue. It is always in the way of A-line detection. In my algorithm, I use time average to deal with them. In Figure10, the left is the orig-

inal frame, we can see that speckle noise generates a lot of tiny horizontal lines which may be wrongly regarded as A-lines during A-line detection. But after combining several adjacent frames together and taking an average of them, we can easily get rid of it.

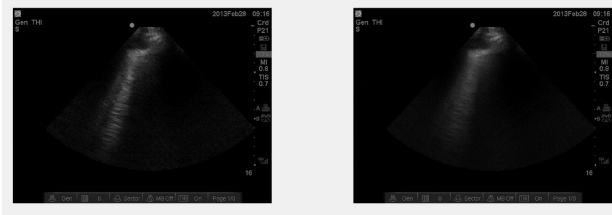


Figure 10: The original noisy frame (left) and the denoised frame (right)

### 3.4 Normalizing

Due to the different gains in different videos, it is hard for us to use a constant threshold directly in the upcoming processing. So, we need to normalize every video at first. Assume that the original brightness of a point is  $A$ , there are two different gains  $G1, G2$ . Then we will get two different outputs  $AG1$  and  $AG2$ . In my algorithm, I try to use the brightness of the pleural line (always the brightest area in a frame) as a standard to normalize them. Assuming the brightness of pleural line is  $S$ , then outputs will be  $SG1$  and  $SG2$ . After normalizing, we will get the same answer,  $\frac{A}{S}$ . Figure 11 will give you a direct impression, and the way to locate the pleural line will be discussed in next chapter.

## 4 Image Segmentation

We follow the guideline that has been discussed before and separate this Chapter into three sections. In the first section, based on some properties of pleural line, we introduce two different methods to determine the location of pleural line. To calculate the ratio of B-lines to rib space, pleural lines' width is used to define the rib space width. In the second section, B-lines are segmented by intensity-based method, and

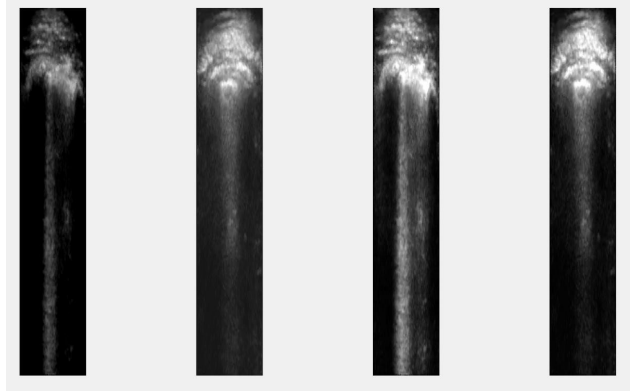


Figure 11: The first and second pictures are original frames with different gains, the third and fourth pictures are normalized frames. It can be seen that the last two frames' intensity distributions are not affected by the gain any more.

in the last section, for the sake of eliminating the wrong B-lines, which contain one or more A-lines, A-line detection is also performed.

### 4.1 Pleural Line Segmentation

Commonly speaking, pleural line is the brightest area in the thorax ultrasound image, so it seems easy for us to locate it. In practice, however, there are several problems making things harder. First is the instability of probes, this will cause the pleural line moving from frame to frame. Locating pleural line for every frame needs a lot of computation and strongly influences the speed of algorithm. Fortunately, the movement is always very slight, so in my algorithm, I take average on all frames from the whole video to locate the pleural line. It works well and will be shown in the picture at the end of this chapter. Second is the number of pleural lines. Generally, for every video, there is always one pleural line located at the middle of the fan area, just between two rib lines. This means that doctors always put the probe between two of our ribs. But sometimes, doctors may put the probe on a rib. In that case, we may see two pleural lines locating at the two sides of the fan area. In my algorithm,

it will just locate one of the two pleural lines. Furthermore, Doctor Rose said that this problem is due to the wrong operation of ultrasound technologist, so we only need to focus on videos with one pleural line. Third is the pattern of the pleural lines. A pleural line is typically a bright thin line in the fan area, but in some of the examples, the brightest areas do not look like a line due to fat and some other tissues as shown in Figure12. From the picture, the pleural is at the bottom of the brightest area.

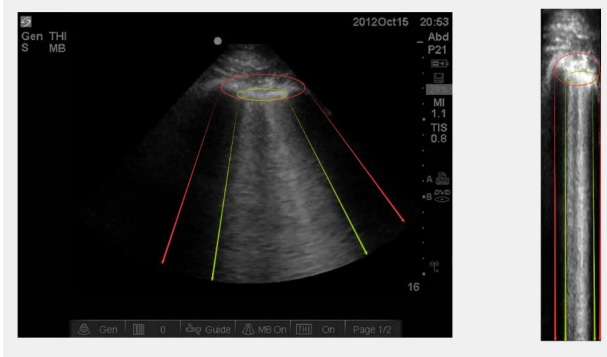


Figure 12: If we just use the total brightest area to decide pleural lines, what we get is the area between red arrows. The correct answer, however, is the area between green arrows.

#### 4.1.1 Region Growing

Region Growing is a simple region-based image segmentation method. It is also classified as a pixel-based image segmentation method since it involves the selection of initial seed points. Rolf Adams and Leanne Bischof [3] created a Seeded Region Growing algorithm, which is based on the conventional region growing postulate of similarity of pixels within regions. The algorithm starts from a set of seeds, which also can be treated as a set of regions; then it compares the intensity value along the boundary of each region to the mean intensity value of this region and label the pixel that satisfied a predefined criterion to update the boundary of the region and the mean value of region intensity value; this process is repeated until no new pixels are added to the region

labelled. Finally, we can get a region that has similar intensity value. The criterion is defined as that the difference between intensity value of the boundary pixels and the mean value of the region's intensity is less than a constant threshold  $e$ . In my algorithm, I search the max value along the brightest area in Figure13 to set the initial seed of growing. And the threshold  $e$  is set as 30, Figure13 is the result of region growing.



Figure 13: Original frame and the result of region growing

There are two problems for region growing. First, the threshold  $e$  is hard to set. In fact, during the test, some of the frames require a small threshold at around 7, but other frames may require a large threshold like 45. So, I can't find a universal threshold for all the frames even after normalization. Second, the solution of region growing does not fit pleural well. Figure13 is the region growing result of the image in Figure12, and, as you can see, the solution of region growing is more likely to regard the red area in Figure12 as a pleural line rather than the green area.

#### 4.1.2 Intensity-based Local Peak Searching

After getting the rectified image, we compute vertical projection by simply adding the value of each pixel in same column directly. Then, in order to eliminate small gap, dilation and erosion are applied on the projection solution, which is shown in Figure14.

In the algorithm, it searches the local peak from 180 to 0, because there won't be a pleural line locat-

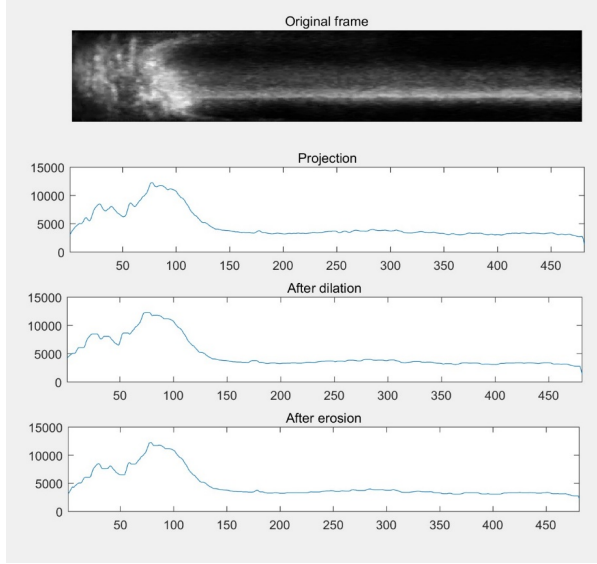


Figure 14: Vertical projection

ing above 200. In fact, they always occur at around  $x = 100$ . The algorithm will pinpoint pleural line by following logic: The value of the local peak must be larger than the value of the right adjacent point and not less than the value of the left adjacent point. The value of the local peak must be not less than 90% of the global maximum value. The algorithm will choose the first local peak meeting the prerequisite from right to left. For example, my algorithm will locate pleural line at  $x = 95$  for Figure14. Next, we need to measure the thickness of the pleural line. We choose a relatively strict constraint to get a thin line but not a mass (for example, the result of region growing algorithm). In my algorithm, it searches the value of points from local peak to left and right, until the function is going to increase or the value is less than 90% of the value of the local peak. For the above example, my algorithm comes up with the boundary coordinate [93,104]. Then, we need to detect the width of pleural line. It is similar to the way we depict above, just do projection on the pleural line area ([93,104]) horizontally. What we will get is shown in Figure15.

Combine results on two different directions, we can

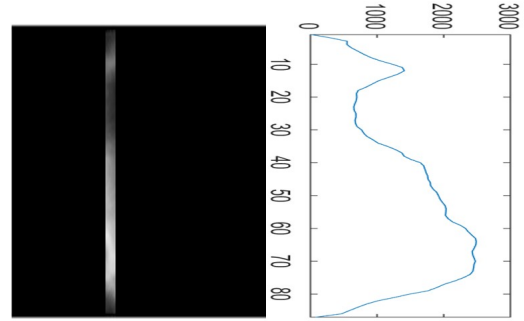


Figure 15: Projection area and projection result

finally locate pleural line. Figure16 is the solution using the same video of above example. To compensate for the slight motion of the pleural line, I extend the width of pleural line by 20% (10% for each side, shown in Figure17). Assuming the width of B-line is  $b$ , the width of pleural line is  $p$ . The B-line occupancy should be  $\frac{b}{p}$ , but due to the motion of the pleural line, it may hard to totally figure out B-line in a whole video. The algorithm extends  $p$  to  $P = 1.2 \times p$  to guarantee that it can always figure out B-line completely. After that, we can still approach the real B-line occupancy by  $1.2 \times \frac{b}{P} = \frac{b}{p}$ . So, this method will only improve the accuracy of my algorithm.

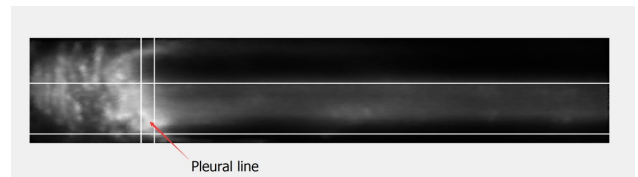


Figure 16: Pinpoint the pleural line

## 4.2 B-line Detection

After identifying pleural line, we can just detect B-line in pleural space. A direct way is to do projection horizontally and use a threshold to figure out B-lines. But in my algorithm, it only uses the right part of the



Figure 17: Pleural line after extending

pleural space to project, shown in Figure18. Recall the definition of B-line: a vertical, comet-tail artefact arising from the pleural line and spreading up to the edge of screen, so we won't lose any B-line. On the other hand, this method can help my algorithm avoid a lot of strange patterns, like Figure19, which is very bright at the left part of the pleural space but totally black at right part of the pleural space.

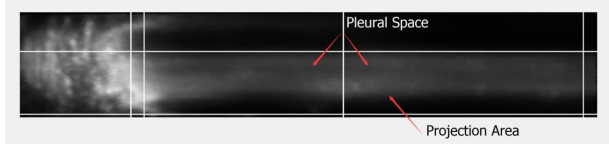


Figure 18: Projection area

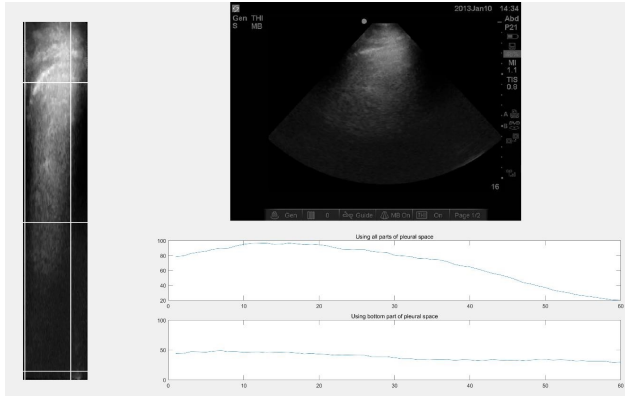


Figure 19: If using whole pleural space to do projection, you may come up with a relatively high solution and wrongly detect a B-line

The frames we process have been normalized in the previous step, so we can use a constant threshold to detect B-lines. In my algorithm, the threshold is 64

(25% of the highest value), so it will regard locations with the average intensity higher than 64 as locations of B-line.

### 4.3 A-line Detection

After we have preliminary detected B-lines, we still need to make sure the existence of A-lines. A-line can locate at the whole area of the pleural space, so we need to check the total area but not the bottom part of the pleural space. Because we just want to make sure there is no A-line lying on detected B-lines, so we just need to exam the existence of A-line on B-line area which has been figured out in the previous section. Due to the speckle noise (which will cause the projection function having a lot of small gaps) and the variable patterns of A-lines (The width of A-line is unsure, this is shown in Figure21), it is difficult to use first order derivative of the projection function to detect A-lines reliably. In my algorithm, it calculates the difference between the base line and the smooth version of projection to detect A-line. Details are shown in Figure20.

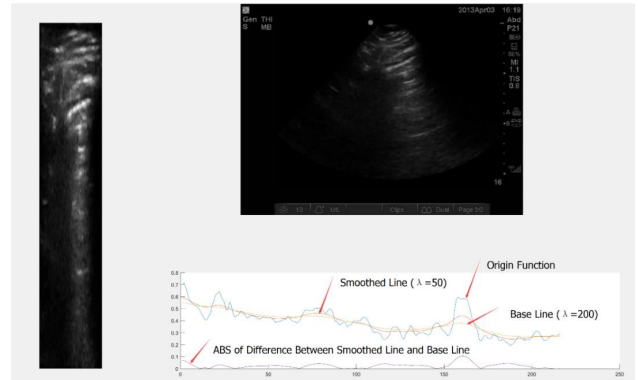


Figure 20: The difference between smoothed line and base line depicts the location of A-lines accurately

My algorithm uses the following method to smooth the project function. Matrix  $Y$  is the input function, matrix  $X$  is the smoothed output function, matrix  $D$  is derivative matrix and  $\lambda$  is a weight parameter. So, the following method tries to minimize the difference between the input and output, as well as the first

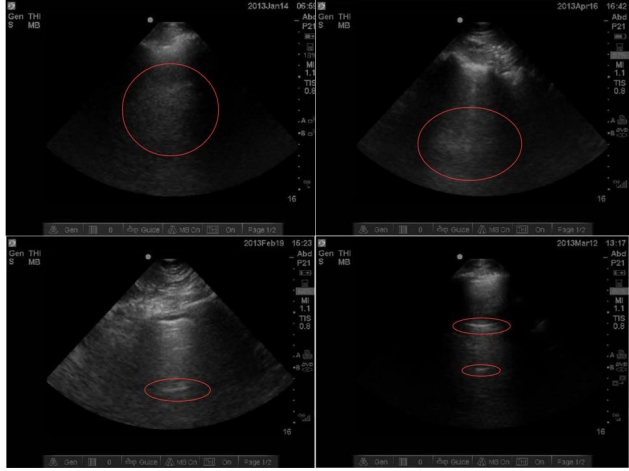


Figure 21: Some of A-lines are bright thin lines (bottom two) and easy to be detected by derivative, but some of A-lines are relative fatter and darker (top two), these A-lines are hard to be detected by derivative.

derivative of the output.

$$\min_X |Y - X|_2 + \lambda |DX|_2 \quad (8)$$

$$X = (I - \lambda D^T D)^{-1} D^T Y \quad (9)$$

If the absolute value difference is higher than 0.05, it will be marked as an A-line.

#### 4.4 ABP-line Map Generation

Once we can detect pleural line, A-line and B-line in a single frame, we can apply the algorithm to a whole video and generate a ABP-map, shown in Figure22. In the left part of Figure22, green lines represent the horizontal location and width of pleural line, red area represents the horizontal location and width of B-lines, blue area represents the existence of A-lines. In the right part of Figure22, the white area represents the vertical location of A-lines.

To eliminate the accidental mistake, we apply dilation and erosion on blue and red area, solution is shown in Figure23.

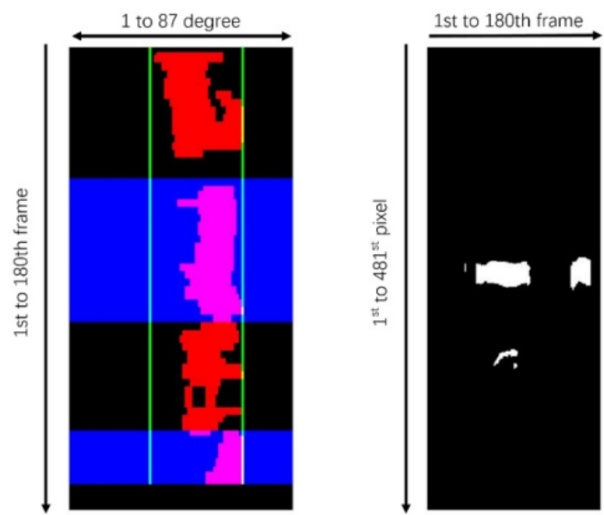


Figure 22: ABP-line Map

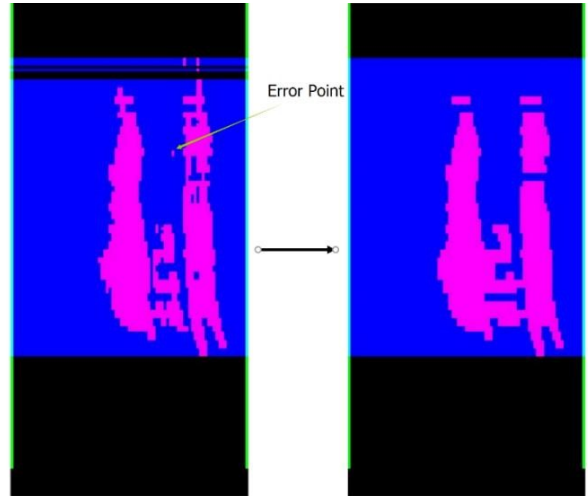


Figure 23: Dilation and Erosion to Eliminate Error

## 4.5 B-line Occupancy

After generating ABP-map, we can calculate the ratio of B-line occupancy. Assuming  $B$  is the summation of the value of B-line area (red area without blue line in Figure??),  $A$  is the total area of the pleural space (the area between green lines), B-line occupancy is equal to  $\frac{B}{A}$ . For each video, it always has 180 frames, so my algorithm will get 180 B-line occupancy values. These values sometimes have a big difference between each other. The reason can be the breath of patient, the shacking of the ultra sound probe or even directing to a wrong direction at first several frames. In that case, averaging directly may not a good method to get a dependable solution. After discussing with Doctor Rose, I decide to using deciles of the total values as the final output.

## 5 Numerical Results

### 5.1 B-line Detection Results

The algorithm finally produces a new video which marks the area of pleural line, B-line and A-line very well. We now have 48 patients, for each patient we have 8 videos coordinating to 8 different places of their lungs, so we finally get 384 output videos. Figure24 shows some of the frames from videos. Doctor Rose is satisfied with the accuracy of the algorithm.

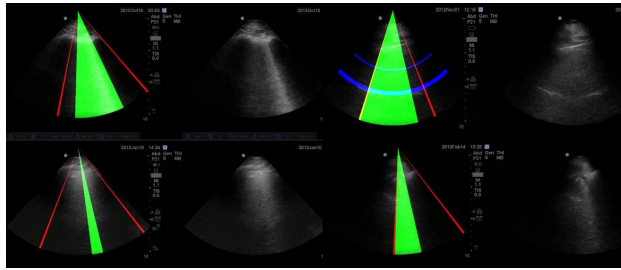


Figure 24: The result of the algorithm

In the test, we have totally 48 patients, each of them has 8 videos according to 8 different parts of his lung. So, we totally have  $48 \times 8 = 364$  videos. My algorithm works well on most of the patients, but

there are still 8 of the 48 patients or 11 of the 364 videos have some problem. The following are some of the reason:

1. 4 videos have some operational mistakes. Such as directing the ultrasound probe to a wrong direction (like liver), shacking probe strenuously
2. 4 videos have local gain but not global gain, and the local gain is too large. That means the brightness and the white noise at some part of the ultrasound video are higher than other parts'. So, my algorithm can't normalize the video correctly
3. 2 videos B-lines pattern are too strange, which may cause by high global gain or improper operations



Figure 25: Abnormal pattern



Figure 26: Operational mistake

### 5.2 Dice Index

I also calculate the dice index of my results. For the correct results, the dice indexes were set to 1, for the



Figure 27: High local gain at the bottom of the fan area

incorrect index I check the real degrees of the B-line and the solutions of my algorithm to calculate the dice index, Figure28 will show these in detail.



Figure 28: The dice index for this example is  $\frac{2a}{b+a}$

After taking an average on all the dice indexes, the dice index for my algorithm is 99.6%. Furthermore, if I exclude the errors stating above (abnormal pattern, local gain or operational mistakes) the dice index will be nearly 100%.

## 6 Future Perspectives and Summary

In the next stage, we plan to:

Get more standard data set, so that my algorithm can get rid of the influence of operational mistakes

and get higher accuracy (presently, my algorithm makes a lot compensation for these operational mistake input).

Get more information for every video, such as the information of local gain, to reinforce the ability of my algorithm.

Try to evaluate the correlation among some other clinical parameters, such as EVLM or BNP, to find out if there is a direct relationship between them.

This work provides an automatic method to detect and evaluate the B-lines in thorax ultrasound images. The detection results correlate quite well with the results produced by clinicians. By using this method, B-lines can be evaluated anywhere (including extreme environmental conditions with pocket size instruments to detect high-altitude pulmonary oedema), anytime (during dialysis to titrate intervention), by anyone (even a novice sonographer after 1 hour training), and on anybody (since the chest acoustic window usually remains patent when echocardiography is not feasible). It also allows non-invasive detection, in real time, of even sub-clinical forms of pulmonary oedema with a low cost, radiation-free approach. This may produce a safer option to monitor ICU patients and greatly reduce the spending of financial and human resources.

## 7 References

- [1] Eugenio Picano, Patricia A. Pellikka. Ultrasound of extravascular lung water: a new standard for pulmonary congestion. *J. European Heart Journal*, doi:10.1093/eurheartj/ehw164
- [2] Anderson KL, Fields JM, Panebianco NL, Jenq KY, Marin J, Dean AJ. Interrater reliability of quantifying pleural B-lines using multiple counting methods. *J Ultrasound Med* 2013; 23:115-120.
- [3] R. Adams and L. Bischof, "Seeded region growing," *IEEE Trans. Pattern Anal. Machine Interll.*, vol. 16, pp. 641-647, 1994.